



Model predictive control of continuous yeast bioreactors using cell population balance models

Guang-Yan Zhu, Abdelqader Zamamiri, Michael A. Henson*, Martin A. Hjortsø

Department of Chemical Engineering, Louisiana State University, Baton Rouge, LA 70803-7303, USA

Received 16 March 2000; received in revised form 6 June 2000; accepted 13 June 2000

Abstract

Continuous cultures of budding yeast are known to exhibit autonomous oscillations that adversely affect bioreactor stability and productivity. We demonstrate that this phenomenon can be modeled by coupling the population balance equation (PBE) for the cell mass distribution to the mass balance of the rate limiting substrate. An efficient and robust numerical solution procedure using orthogonal collocation on finite elements is developed to approximate the PBE model by a coupled set of nonlinear ordinary differential equations (ODEs). A controller design model is obtained by linearizing and temporally discretizing the ODEs derived from spatial discretization of the PBE model. The resulting linear state-space model is used to develop model predictive control (MPC) strategies that regulate the discretized cell number distribution by manipulating the dilution rate and the feed substrate concentration. Two choices of the controlled output vector are considered: (i) the entire discretized distribution; and (ii) a subset of the discretized distribution. The ability of the MPC controllers to stabilize steady-state and periodic solutions is evaluated via simulation. We show that superior closed-loop performance is obtained when a subset of the distribution is employed as controlled outputs. © 2000 Elsevier Science Ltd. All rights reserved.

1. Introduction

Saccharomyces cerevisiae (Baker's yeast) is an important microorganism in a number of industries including brewing, baking, food manufacturing and genetic engineering. Under routine operating conditions, continuous bioreactors producing *Saccharomyces cerevisiae* can exhibit autonomous and sustained oscillations (Strässle, Sonnleitner & Feichter, 1989b). The oscillations eventually disappear, presumably due to external disturbances or deficiencies in the medium. Similar oscillations have been observed in other continuous microbial cultures (McLellan, Daugulis & Li, 1999). In most situations, oscillations adversely affect bioreactor operability and the objective is to eliminate the limit cycle behavior by stabilizing a chosen steady state. On the other hand, it may be desirable to induce and stabilize oscillations to increase the production of metabolites that are produced during a certain phase of the cell cycle (Hjortsø & Bailey,

1983). To achieve these objectives, it is necessary to derive a dynamic model that describes the oscillatory behavior and to develop a control strategy that allows modification of the intrinsic reactor dynamics.

The mechanisms responsible for sustained oscillations in *Saccharomyces cerevisiae* cultures are controversial and a subject of current research. The oscillatory behavior has been modeled by segregated structured models (Cazzador, Mariani, Martegani & Alberghina, 1990; Strässle, Sonnleitner & Feichter, 1989a), segregated unstructured models (Hjortsø & Nielsen, 1994) and metabolic (cybernetic) models (Jones & Kompala, 1999). Unsegregated (also known as distributed) models are based on the assumption of a continuous and well-mixed biophase, while segregated models treat the biophase as a population of cells with different properties. Unstructured models have no chemical structure imposed on the biophase, while structured models are based on an assumed chemical structure. Segregated structured models are capable of representing a broad range of cell mechanisms. However, parameter identification and numerical solution of such models are very difficult due to the large number of variables involved. Moreover, Beuse, Bartling,

* Corresponding author. Fax: 225-388-1476.

E-mail address: henson@che.lsu.edu (M. A. Henson).

Kopmann, Diekmann and Thoma (1998), show that the assumption of certain cell classes may lead to a structured segregated model (Strässle et al., 1989a) that cannot model experimentally observed changes of cell subpopulations over a range of dilution rates. In this paper, a segregated unstructured model is proposed because this is perhaps the simplest model form that is able to predict periodic behavior of the cell population and its relation to cell cycle synchrony (Hjortso & Nielsen, 1994, 1995).

Cybernetic models explain oscillations via metabolic events such as the competition between glucose oxidative and fermentative pathways (Jones & Kompala, 1999). Due to their unsegregated nature, this class of models cannot directly explain cell synchronization (i.e. the formation of distinct cell subpopulations) that accompanies the oscillations (Chen & McDonald, 1990). Instead, cell cycle synchrony is assumed to be a consequence of the metabolic oscillations. Our previous work (Hjortso, 1987) shows that induction synchrony can occur only when the period of the metabolic forcing is equal to the period of the cell cycle. Consequently, metabolic models resort to a coincidental match of the metabolic and cell cycle periods to explain the observed cell cycle synchrony. As discussed in Section 2, we believe that segregated unstructured models based on population balance equations provide a more realistic description of the cell cycle events that lead to sustained oscillation in budding yeast cultures.

Although there exists a large number of papers on modeling of particulate systems, the literature on particulate system control is much more sparse. Controllability issues for population balance equation (PBE) models are studied by Semino and Ray (1995a). The analysis results are used to design single-input–single-output control strategies that eliminates oscillatory behavior in an emulsion polymerization reactor (Semino & Ray, 1995b). Rawlings and co-workers design model-based controllers that allow regulation of the crystal size distribution in continuous crystallizers (Eaton & Rawlings, 1990; Rawlings, Witkowski & Eaton, 1989). Feedback linearizing control strategies based on moment models of continuous crystallizers are proposed by Chiu and Christofides (1999).

In this paper, a linear model predictive control (LMPC) strategy based on a spatially discretized PBE model is proposed for the stabilization of oscillating yeast cultures. Cell mass is used as the internal cell coordinate to facilitate real-time measurement of the cell number distribution. The linear state-space model used for LMPC design is obtained by linearizing and temporally discretizing the nonlinear ordinary differential equations resulting from spatial discretization of the PBE model. The LMPC strategy is designed to allow stabilization of steady-state and periodic solutions via direct control of the cell mass distribution.

The rest of the paper is organized in four sections. In Section 2, previous work on PBE modeling and control of oscillating microbial culture is reviewed and compared with the present contribution. The PBE model is presented in Section 3 along with the numerical solution procedure for the resulting set of partial differential/integral equations. In Section 4, the LMPC strategy is presented with special emphasis on the use of the discretized cell mass distribution as controlled outputs. Closed-loop simulation results for the attenuation and induction of oscillations also are shown in Section 4. Finally, a summary is given in Section 5.

2. Previous work on oscillating microbial cultures

Our previous models for oscillating microbial cultures (Hjortso & Nielsen, 1994, 1995) involve coupling the population balance equation (PBE) for the cell age distribution to the substrate mass balance. The simplified cell cycle used in the derivation of the PBE model for budding yeast cultures is shown in Fig. 1. The cell cycle has two control points: (i) the transition age (a_t) when a daughter cell becomes a mother cell capable of undergoing budding; and (ii) the division age (a_d) when the budding mother cell produces a daughter cell. The assumption of discrete control points is a simplification of the probabilistic division properties of real yeast cells. The control points are influenced by medium composition, especially the concentration of the rate limiting substrate. The coupling of the PBE and the substrate balance equation establishes an internal feedback loop that can induce sustained oscillations. The basic mechanism can be explained as follows. A partially synchronized cell culture produces periodic changes in the medium, which in turn induces periodic changes in a_t and a_d . This leads to further synchronization of the culture and ultimately results in sustained oscillations. A detailed

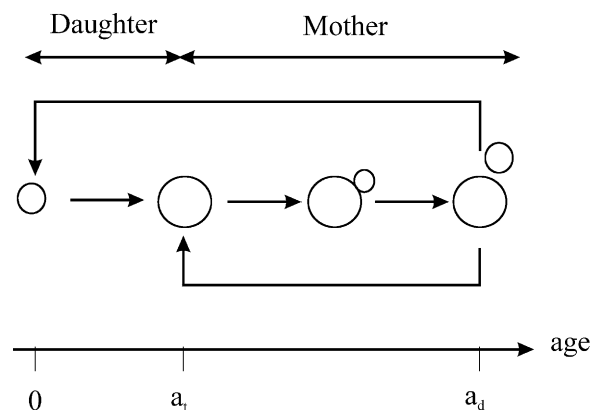


Fig. 1. Cell cycle for budding yeast used in deriving cell age distribution models.

description and analysis of this PBE model can be found in Hjortso and Nielsen (1994, 1995).

In our previous work on binary fission organisms (Kurtz, Zhu, Zamamiri, Henson & Hjortso, 1998), the PBE model has been enhanced by replacing the discrete division control point with a division intensity function $\Gamma(a, S')$, where a is the cell age and S' is the “effective” substrate concentration. The function $\Gamma(a, S')$ represents the specific rate of cell division at age a and approaches infinity as the cell age approaches some critical value $a_c(S')$. The effective substrate concentration (S') is introduced to describe the delayed response of cell metabolism to changes in environmental conditions and is modeled as a filtered value of actual substrate concentration. These enhancements provide a more realistic description of cell cycle behavior than the conceptual models in Hjortso and Nielsen (1994, 1995). The resulting PBE model has been used as the basis for the development of a feedback linearizing control strategy. Rather than control the cell number distribution as in the present work, the nonlinear controller design is based on a simplified moment representation of the PBE model. Additional details can be found in Kurtz et al. (1998).

Although it is natural to use cell age as the internal coordinate for PBE modeling of microbial cultures, there are complications associated with age domain models with respect to model-based controller design. In particular, the cell age distribution cannot be measured directly and it is difficult to develop an useful mapping between the age distribution and the cell size distribution. With recent developments in particle measurement technology (Heffels et al., 1998; Rawlings, Miller & Witkowski, 1993; Yamashit, Kuwashim, Nonaka & Suzuki, 1993), the particle size distribution now can be measured on-line. However, cell size is not a convenient internal coordinate for microbial cultures due to the difficulties associated with deriving cell size models. It is possible to establish a mapping between the cell mass distribution and the cell size distribution. Such mappings can be developed for certain microbial cultures with the knowledge of the cell density, dry-matter content and cell geometry (Bakken & Olsen, 1983). By using flow cytometry to analyze forward light scatter intensity that varies with bacteria dry mass, a method for determining biomass distribution in mixed bacterial population is reported in Robertson, Button and Koch (1998). In this paper, we use cell mass as the internal coordinate for deriving the PBE model and assume the cell mass distribution is measured.

3. PBE model development and numerical solution of the PBE model

3.1. Model development

The PBE model employed in this paper contains several enhancements of the models used in our previous

works (Hjortso & Nielsen, 1994; Kurtz et al., 1998). First, the binary fission culture studied in Kurtz et al. (1998) is replaced by a budding yeast culture with the more complex cell cycle that depicted in Fig. 1. Second, cell mass is used as the internal coordinate rather than cell age as in Hjortso and Nielsen (1994) and Kurtz et al. (1998). Third, the generation of newborn cells is modeled by a Gaussian-like probability function rather than by discrete control points as in Hjortso and Nielsen (1994). Fourth, cell division and transition are affected by a filtered substrate concentration rather than a purely delayed substrate concentration as in Hjortso and Nielsen (1994).

The PBE is written as

$$\begin{aligned} \frac{\partial W(m, t)}{\partial t} + \frac{\partial [k(S')W(m, t)]}{\partial m} \\ = \int_0^{m'} 2p(m, m')\Gamma(m', S')W(m', t) dm' \\ - [D + \Gamma(m)]W(m, t), \end{aligned} \quad (1)$$

where $W(m, t)$ is the number density of cells with mass m at time t , $k(S')$ is the single cell growth rate, S' is the effective substrate concentration, $p(m, m')$ is the probability that a newborn cell of mass m is produced from a mother cell dividing at mass m' , $\Gamma(m, S')$ is the division intensity function, and D is the dilution rate. The initial condition of the cell mass distribution is denoted as $W(m, 0)$.

The division intensity function $\Gamma(m, S')$ models the tendency of budding cells to divide as they approach a certain critical mass. The function is assumed to have the form

$$\Gamma(m, S') = \begin{cases} 0, & m \leq m_i^* + m_o, \\ \gamma \exp[-\varepsilon(m - m_d^*)^2], & m_i^* + m_o < m < m_d^*, \\ \gamma, & m \geq m_d^*, \end{cases} \quad (2)$$

where m_i^* is the transition mass, m_o is the additional mass that mother cells must gain before division is possible, ε and γ are constant parameters and m_d^* is the mass at which the division intensity reaches its maximum value γ . The transition and division masses are functions of S' as discussed later in this section. The parameter ε determines how rapidly the division rate increases as the cell mass approaches m_d^* . The division intensity function is plotted in Fig. 2a for the parameter values listed in Table 1. It is important to note that the parameter values have been chosen to provide reasonable reactor operating conditions. As part of our future work, we intend to investigate the estimation of model parameters from experimental data generated in our laboratory.

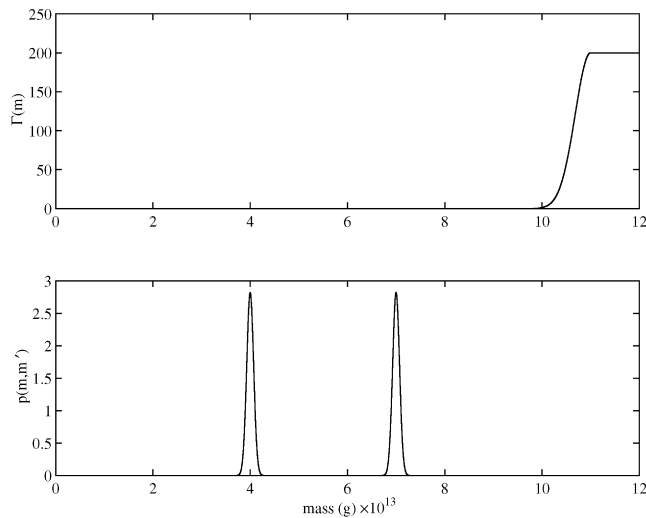


Fig. 2. (a) The division intensity function $\Gamma(m)$; and (b) the newborn cell probability $p(m, m')$ ($m' = 11 \times 10^{-13}$ g, $m_t^* = 7 \times 10^{-13}$ g).

Table 1
Nominal operating conditions

Variable	Value	Variable	Value
γ	200	ε	5
A	$\sqrt{25/\pi}$	β	100
S_l	0.1 g/l	S_h	2 g/l
K_t	0.01	K_d	2
m_{t0}	6×10^{-13} g	m_{d0}	11×10^{-13} g
m_{max}	12×10^{-13} g	m_o	1×10^{-13} g
Y	0.4	μ_m	5×10^{-12} g/h
K_m	25 g/l	α	20
D	0.4 h^{-1}	S_f	25 g/l

The newborn cell probability function $p(m, m')$ describes the mass distribution of newborn cells resulting from cell division. This function is modeled as

$$p(m, m') = \begin{cases} A \exp[-\beta(m - m_t^*)^2] + A \exp[-\beta(m - m' + m_t^*)^2], & m' > m \text{ and } m' > m_t^* + m_o, \\ 0, & m' \leq m \text{ or } m' \leq m_t^* + m_o, \end{cases} \quad (3)$$

where m is the mass of the newborn cell, m' is the mass of the budding mother cell, and A and β are constant parameters. The function $p(m, m')$ is set to zero for $m' \leq m_t^* + m_o$ (when no division can occur) or $m' \leq m$ (which is not physically meaningful). The probability function $p(m, m')$ obviously must satisfy

$$\int_0^{m'} p(m, m') dm = 1. \quad (4)$$

Function (3) yields two identical Gaussian-like peaks in the mass domain, one centered at the substrate-depen-

dent transition mass m_t^* (corresponding to newborn mother cells) and one centered at $m' - m_t^*$ (corresponding to newborn daughter cells). The function $p(m, m')$ is plotted in Fig. 2b for the parameter values in the Table 1.

By incorporating the division intensity function (2) and the newborn cell probability function (3), the PBE model becomes more biologically plausible than conceptual models based on discrete control points (Hjortsø & Nielsen, 1994). However, sustained oscillations are more difficult to generate with the proposed PBE model because $\Gamma(m, S')$ and $p(m, m')$ introduce dispersive effects that tend to counteract the effects of cell synchrony. We have found that the functions used to model the substrate dependence of the transition mass (m_t^*) and the division mass (m_d^*) play important roles in the ability of the model to exhibit stable periodic solutions.

The following saturation functions are proposed for the transition and division masses:

$$m_t^*(S') = \begin{cases} m_{t0} + K_t(S_l - S_h), & S' < S_l, \\ m_{t0} + K_t(S' - S_h), & S' \in [S_l, S_h], \\ m_{t0}, & S' > S_h, \end{cases} \quad (5)$$

$$m_d^*(S') = \begin{cases} m_{d0} + K_d(S_l - S_h), & S' < S_l, \\ m_{d0} + K_d(S' - S_h), & S' \in [S_l, S_h], \\ m_{d0}, & S' > S_h, \end{cases} \quad (6)$$

where S_l , S_h , m_{t0} , m_{d0} , K_t and K_d are constant parameters. Note that both m_t^* and m_d^* are increasing functions of the effective substrate concentration S' . Fig. 3 shows $m_t^*(S')$ and $m_d^*(S')$ for the parameter values in Table 1. These functionalities are in general agreement with experimental data (Alberghina, Ranzi, Porro & Martegani, 1991; Martegani, Porro, Ranzi & Alberghina, 1990) that the transition mass (m_t) and the division mass (m_d) are positive functions of nutritional conditions and that m_d is much more strongly affected than is m_t . The ratio of the division and transition masses is reported to

be 1.6–1.7 at good nutritional conditions and 1.15–1.2 at poor nutritional conditions (Alberghina et al., 1991; Martegani et al., 1990). For the parameters in Table 1, the ratio of m_d^* and m_t^* is 1.8 for $S' \geq 2$ g/l and 1.5 for $S' \leq 0.01$ g/l. Since the division mass (m_d) is less than the critical division mass m_d^* , these ratios appear to be in reasonable agreement with published data.

The substrate balance is written as

$$\frac{dS}{dt} = D(S_f - S) - \int_0^\infty \frac{k(S')}{Y} W(m, t) dm, \quad (7)$$

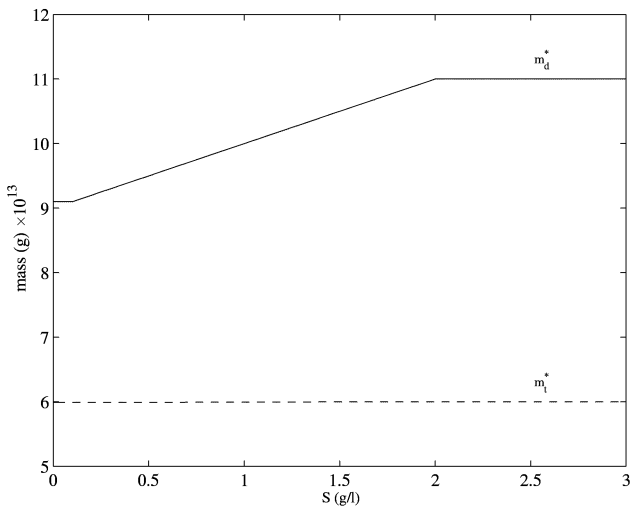


Fig. 3. The division mass $m_d^*(S')$ (—) and the transition mass $m_t^*(S')$ (---).

where S is the actual substrate concentration, S' is the effective substrate concentrations, S_f is the feed substrate concentration and Y is a constant yield coefficient. The single cell growth rate is assumed to follow simple Monod kinetics:

$$k(S') = \frac{\mu_m S'}{K_m + S'} \quad (8)$$

where μ_m and K_m are constant parameters. The filtered substrate concentration is calculated as

$$\frac{dS'}{dt} = \alpha(S - S'), \quad (9)$$

where the constant parameter α determines how rapidly cells respond to environmental changes (Stephens & Lyberatos, 1987).

As compared to conceptual models with discrete control points (Hjortso & Nielsen, 1994), the dynamic behavior of the proposed PBE model is more complex due to the incorporation of the filtered substrate concentration S' and the functions $\Gamma(m, S')$ and $p(m, m')$. These functions tend to create dispersive effects that counteract cell synchronization that leads to sustained oscillations. As shown below, the proposed model is capable of generating stable periodic solutions via the internal feedback mechanism described in Hjortso and Nielsen (1994). A partially synchronized cell population induces periodic changes in the substrate concentration, which then leads to periodic changes in the transition and division masses. These two variables determine the mass of dividing mother cells and newborn daughter cells and therefore impose upper and lower bounds on the cell state space. Periodic changes in these boundaries create a stable attractor that overcomes the dispersive effects.

3.2. Numerical solution

The PBE model is comprised of a coupled set of nonlinear algebraic, ordinary differential and integro-partial differential equations. Analytical solution of such models is possible only under very restrictive assumptions (Hjortso & Nielsen, 1994, 1995). Consequently, numerical solution is required when the PBE model is used in open- and closed-loop simulations. In our previous work on binary fission organisms (Kurtz et al., 1998), the PBE model is solved using a finite difference method. This method is simple to implement, but it is computationally inefficient and less accurate than alternative techniques based on weighted residuals (Finlayson, 1980).

We have found that orthogonal collocation on finite elements (Finlayson, 1980) provides efficient and robust solution of the PBE model. A finite cell mass domain, $0 \leq m \leq m_{\max}$, is chosen such that the number of cells with mass $m > m_{\max}$ is negligible. The PBE is approximated by a coupled set of nonlinear ordinary differential equations (ODEs) that are obtained by discretizing the mass domain. Integral expressions in the population and substrate balance equations are approximated using Gaussian quadrature (Finlayson, 1980). The resulting set of nonlinear ODEs has the form

$$\begin{aligned} \frac{dW_j}{dt} = & -\frac{1}{h}k(S') \sum_{i=1}^n A_{j,i} W_i + h \sum_{i=1}^n 2w_i P_{j,i} \Gamma_i W_i \\ & - (D + \Gamma_j) W_j, \quad j = 1, 2, \dots, n, \end{aligned} \quad (10)$$

$$\frac{dS}{dt} = D(S_f - S) - \frac{k(S')}{Y} h \sum_{i=1}^n w_i W_i, \quad (11)$$

$$\frac{dS'}{dt} = \alpha(S - S'), \quad (12)$$

where W_j denotes the cell number density at collocation point j , n is the total number of collocation points, A is the collocation matrix (Finlayson, 1980), h scales the size of each finite element to unity; w is a vector of quadrature weights (Finlayson, 1980), $P_{j,i} = p(m_j, m_i)$ is the (i, j) element of the matrix $P \in R^{n \times n}$, and $\Gamma_i = \Gamma(m_i)$ is i th element of the vector $\Gamma \in R^n$. Both P and Γ are time varying because they are dependent on S' . Unless stated otherwise we use 12 equally spaced finite elements, each with eight internal collocation points that are determined as the roots of the appropriate Jacobi polynomial (Rice & Do, 1995). The total number of collocation points $n = 109$. The state vector of the resulting ODE model consists of the cell number density at each collocation point (W_j), as well as the substrate and filtered substrate concentrations (S, S').

The accuracy of the proposed numerical solution procedure is evaluated by: (i) using a simplified model to compare the numerical solution to an analytical solution; (ii) and testing convergence of the numerical solution using different number of collocation points. An analytical solution of the PBE model can be obtained via the method of characteristics (Hjortsø & Bailey, 1983) under the following assumptions:

1. Constant single cell growth rate.
2. Constant division and transition masses.
3. Infinite division intensity at the division mass.

The assumption of constant cell growth decouples the PBE from the substrate balance equation. The assumption of discrete division and transition masses leads to distinct mother (M) and daughter (D) cell populations. The PBE model is written for the two subpopulations as follows:

$$\frac{\partial W_M(m, t)}{\partial t} + k \frac{\partial W_M(m, t)}{\partial m} = -DW_M(m, t), \quad (13)$$

$$\frac{\partial W_D(m, t)}{\partial t} + k \frac{\partial W_D(m, t)}{\partial m} = -DW_D(m, t), \quad (14)$$

where W_M and W_D are the cell number concentrations of mother and daughter cells, respectively, and k is the constant single cell growth rate. Due to the infinite division intensity assumption, cell division is incorporated into the boundary conditions:

$$W_M(m_t, t) = W_M(m_d, t) + W_D(m_t, t), \quad (15)$$

$$W_D(m_o, t) = W_M(m_d, t), \quad (16)$$

where m_d is the constant division mass, m_t is the constant transition mass and m_o is the constant minimum cell mass.

Using the method of characteristics, the PBEs for the mother and daughter cell populations are solved in subdomains defined by characteristic curves with slopes of the growth rate k . Fig. 4 shows a comparison of the numerical and analytical solutions for the cell number distributions. The dilution rate is 0.25 h^{-1} , and the single cell growth rate is $k = 4 \times 10^{-13} \text{ g/h}$. The minimum cell mass, transition mass and division mass are $m_o = 4 \times 10^{-13} \text{ g}$, $m_t = 8 \times 10^{-13} \text{ g}$, $m_d = 12 \times 10^{-13} \text{ g}$, respectively. The following initial distributions are used:

$$W_M(m, 0) = 0, \quad (17)$$

$$W_D(m, 0) = 10^{13} e^{-5(m - 6 \times 10^{-13})^2}. \quad (18)$$

For this simple model, eight finite elements and five internal collocation points are found to be sufficient for numerical solution. The difference between the analytical and numerical solutions is obtained by interpolating the analytical solution to match the mass-time grid used for numerical solution. The results in Fig. 4 demonstrate that the numerical solution provides a very close approxima-

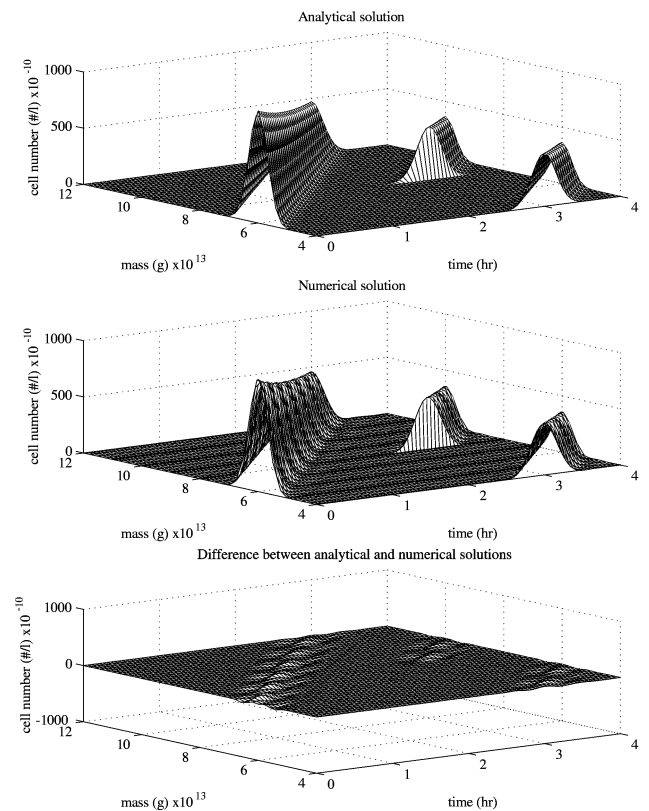


Fig. 4. Analytical and numerical solutions of the simplified PBE model.

tion of the analytical solution. Note that only the first three subdomains for the daughter and mother cells are solved analytically due to the increasingly complex expressions obtained for higher subdomain solutions (Hjortsø & Bailey, 1983).

From a conceptual standpoint, an advantage of the simplified model is that the cell cycle can be easily visualized. Fig. 5 shows the numerical solution of the simplified model for the same test as in Fig. 4 but with a longer time duration of 8 h. Note that discontinuities are observed due to the assumption of discrete control points. Budding mother cells divide into daughter cells and new mother cells when the mass $m = m_d = 12 \times 10^{-13} \text{ g}$. At the cell transition mass $m_t = 8 \times 10^{-13} \text{ g}$, the new mother cell density $W_M(m_t, t)$ is the sum of the daughter cell density $W_D(m_t, t)$, and the density of dividing mother cells $W_M(m_d, t)$ as in (15). Similarly, the density of daughter cells with mass m_o equals the density of cells divided as in (16). Because discrete control points are used and cell growth is independent of the medium, the shape of the cell distribution is invariant with respect to time within the same cell cycle and the total number of cells decreases.

Analytical solution of the detailed PBE model in (1)–(9) is not possible. In the remainder of the paper, the model is solved numerically using 12 finite elements and eight internal collocation points. An appropriate number

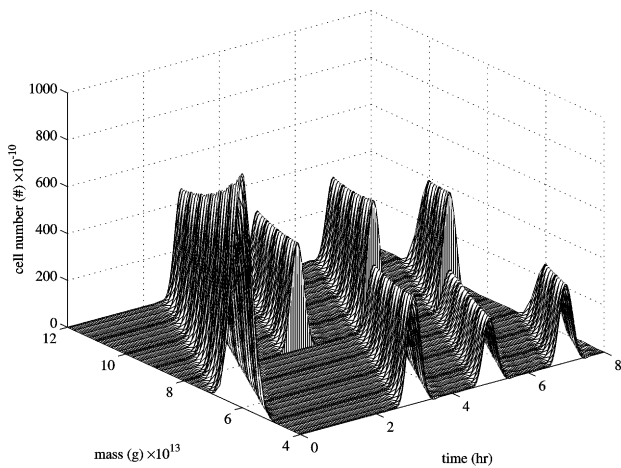


Fig. 5. Numerical solution of the simplified PBE model.

of internal collocation points (n_c) is chosen by performing a series of open-loop simulation tests with $n_c = 6, 8$ and 9 to check convergence of the numerical solution. The results for the initial cell number distribution (17) and (18) and two sets of operating conditions are shown in Fig. 6. An oscillatory response is obtained for $D = 0.25 \text{ h}^{-1}$ and $S_f = 20 \text{ g/l}$. This result indicates that $n_c = 8$ is sufficient to obtain an accurate solution. A steady-state solution is obtained with a larger dilution rate $D = 0.4 \text{ h}^{-1}$ and a larger feed substrate concentration $S_f = 25 \text{ g/l}$. The corresponding substrate concentration dynamics also are shown in Fig. 6. These results are consistent with experimental data (Zamamiri, 1998).

4. Model predictive controller design

The budding yeast PBE model is difficult to use directly for model-based controller design. A reasonable alternative is to use the PBE model to derive simpler ODE models that are more amenable to existing controller design techniques. Moment models have been developed for particulate systems such as continuous crystallizers (Chiu & Christofides, 1999) and aerosol reactors (Kalani & Christofides, 1999). The moments of the distribution can be used as controlled outputs. For such particulate processes, closed-form representation of the moment equations is possible because new particle generation depends only on lumped variables (e.g. initiator and monomer concentrations in emulsion polymerization). In Kurtz et al. (1998) it is shown that binary fission organisms do not allow closure of the first- and higher-order moments because the birth rate of new cells always depends on the cell distribution. A similar problem occurs for the budding yeast PBE model.

In our previous work on binary fission organisms (Kurtz et al., 1998), a zeroth-order moment model is used

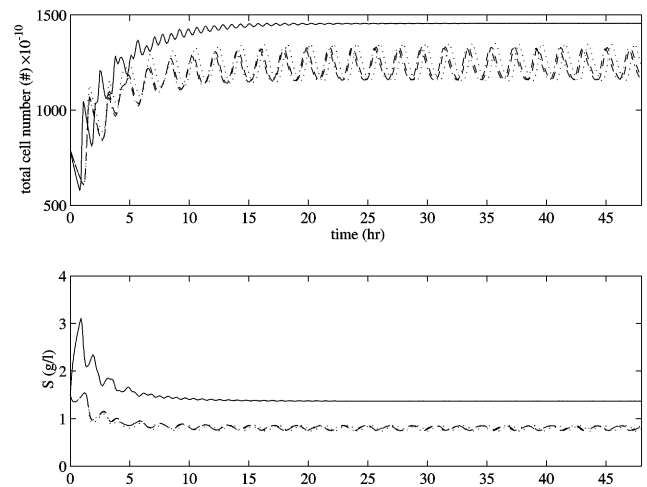


Fig. 6. Open-loop simulation: steady-state solution with $n_c = 8$ (—) and oscillatory solutions with $n_c = 6$ (⋯), $n_c = 8$ (---), and $n_c = 9$ (-·-·).

to derive a feedback linearizing controller. A shortcoming of this approach is that the controller design model does not account for the segregated nature of the culture despite the fact that sustained oscillations are intimately connected to cell synchrony. Below we propose a model predictive control strategy for the budding yeast cultures based on a linear design model that preserves the segregated description of the PBE model.

4.1. Controller formulation

The controller design model is generated directly from the spatially discretized PBE model (10)–(12). The model equations are linearized about the steady-state operating point in Table 1 and then temporally discretized with sampling time $\Delta t = 0.1 \text{ h}$. The sampling time is chosen to be an order of magnitude less than the period of the oscillating culture (2 h). The resulting state-space model has the form

$$\begin{aligned} x(k+1) &= Ax(k) + Bu(k), \\ y(k) &= Cx(k), \end{aligned} \quad (19)$$

where $x \in R^{111}$ is the state vector comprised of the cell number density at each collocation point (W_j) and the substrate and filtered substrate concentrations (S, S'); $u \in R^2$ is the input vector comprised of D and S_f ; and $y \in R^m$ is the output vector defined below. As discussed in Section 2, we assume that the cell mass distribution can be measured or reconstructed from on-line measurements of the particle size distribution.

The controllability matrix for the pair (A, B) in (19) has rank four. This is not a surprising result given the large state dimension and the strong colinear behavior of the state variables. This indicates that the cell distribution cannot be modified arbitrarily with the two inputs

available. Semino and Ray (1995a) propose an approximate controllability test for PBE models that can be placed in hereditary form via semi-analytical solution. Controllability is defined as the property that the state vector can be driven from a subspace Γ_1 to a subspace Γ_2 in a finite amount of time by appropriate choice of the inputs. The controllability test is successfully applied to emulsion polymerization reactors and continuous crystallizers. Unfortunately, the test does not appear to be applicable to microbial PBE models because they do not allow the required hereditary system representation. In this paper, we investigate the ability of the MPC controller to stabilize steady-state and periodic solutions. While we consider partial control of the cell distribution, it is unnecessary to precisely establish a given cell distribution to achieve the control objectives (see below).

The controller design model is completed by defining the controlled output vector. The most straightforward approach is to choose the cell number density W_j at each collocation point as a controlled output. This may be problematic because: (i) the resulting control problem is highly non-square (2 inputs, 109 outputs); (ii) cell number densities at nearby collocation points are strongly colinear because the basic shape of the distribution cannot be changed significantly by manipulating D and S_f ; and (iii) the substrate concentration also needs to be controlled to avoid washout. The third problem can be handled by defining the output vector as

$$y = [W_1 \quad W_2 \quad \dots \quad W_N \quad S]^T. \quad (20)$$

We have found that good closed-loop performance can be obtained by controlling a subset of the cell number densities and the substrate concentration:

$$y = [W_{j_1} \quad W_{j_2} \quad \dots \quad W_{j_p} \quad S]^T, \quad (21)$$

where the indices $\{j_1, \dots, j_p\}$ define the collocation points where the associated cell number density is used as a controlled output. In the subsequent simulation study, $\{j_1, \dots, j_p\}$ are chosen as boundary points of the finite elements. While this approach is admittedly heuristic, problems may be encountered if the number of output variables is reduced further. Fewer output variables may not be able to represent the time-varying cell distribution which shifts position as the substrate concentration changes. While it may be possible to systematically determine the controlled outputs using multivariate statistical methods (Clarke-Pringle & MacGregor, 1998), this was deemed to be beyond the scope of the current study. Below we compare the performance of MPC controllers which use the output vectors (20) and (21).

4.2. Controller design

The major control objectives are: (i) stabilization of steady-state solutions to eliminate oscillations that adversely affect bioreactor stability and productivity; and

(ii) stabilization of periodic attractors that may lead to increased production of metabolites synthesized only during part of the cell cycle (Hjortsø, 1996). Both objectives can be achieved by controlling the discretized cell number distribution because oscillatory behavior is closely linked to synchronization of the cell population.

The MPC controller is formulated as an infinite-horizon open-loop optimal control problem (Muske & Rawlings, 1993)

$$\begin{aligned} \min_{U_N(k)} \sum_{j=0}^{\infty} \{ & [y(k+jk) - y_s]^T Q [y(k+jk) - y_s] \\ & + [u(k+jk) - u_s]^T R [u(k+jk) - u_s] \\ & + \Delta u^T(k+jk) S \Delta u(k+jk) \}, \end{aligned} \quad (22)$$

where $y(k+jk)$ and $u(k+jk)$ are predicted values of the outputs and inputs, respectively, y_s and u_s are target values for the outputs and inputs, respectively, and $\Delta u(k) = u(k) - u(k-1)$. The decision variables are current and future values of the inputs: $U_N(k) = [u(k|k) \dots u(k+N-1|k)]$, where N is the control horizon. The inputs are subject to constraints of the form: $u_{\min} \leq u \leq u_{\max}$. The infinite horizon problem (22) can be reformulated as a finite horizon problem and solved using standard quadratic programming software (Muske & Rawlings, 1993). Using the standard receding horizon approach, only the first calculated input actually is implemented, $u(k) = u(k|k)$, and the problem is resolved at the next time step with new measurements.

The target vectors u_s and y_s can be constant or adjusted on-line using a disturbance model. The disturbance model is formulated as follows (Muske & Rawlings, 1993):

$$\begin{aligned} x(k+1) &= Ax(k) + Bu(k), \\ d(k+1) &= d(k), \\ y(k) &= Cx(k) + d(k), \end{aligned} \quad (23)$$

where d is a vector of output disturbance variables. The output disturbance estimate \hat{d} is generated by a Kalman filter (Muske & Rawlings, 1993). As discussed above, there are insufficient degrees of freedom to drive the entire cell distribution to a specified target distribution. Therefore, target vectors x_s and u_s that minimize the steady-state offset are found by solving the following quadratic programming problem (Muske & Rawlings, 1993):

$$\min_{[x_s, u_s]^T} (y_{\text{ref}} - Cx_s - \hat{d})^T R_s (y_{\text{ref}} - Cx_s - \hat{d}) \quad (24)$$

subject to

$$[I - A - B] \begin{bmatrix} x_s \\ u_s \end{bmatrix} = 0, \quad (25)$$

$$u_{\min} \leq u_s \leq u_{\max}. \quad (26)$$

Below we investigate MPC controller designs with and without the disturbance model.

4.3. Simulation study

The proposed MPC strategy is evaluated using the discretized PBE model (10)–(12) as a surrogate for the continuous yeast bioreactor. Two controller formulations are investigated using the alternative output vectors discussed above. The first controller uses the full-order output vector (20). This leads to a highly non-square control problem (2 inputs, 110 outputs) due to the large number of collocation points employed. The quadratic weighting matrices in the objective function (22) are chosen by trial-and-error as

$$Q = \begin{bmatrix} 0.01I_{109 \times 109} & 0 \\ 0 & 10 \end{bmatrix}, \quad R = \begin{bmatrix} 10^5 & 0 \\ 0 & 100 \end{bmatrix},$$

$$S = 2R. \quad (27)$$

A control horizon $N = 5$ provides a reasonable compromise between closed-loop performance and computation time. The second controller uses the reduced-order output vector (21). This yields a lower dimensional problem with 14 output variables. The control horizon is chosen as $N = 5$ and the weighting matrices are chosen by trial-and-error as

$$Q = \begin{bmatrix} 0.1I_{13 \times 13} & 0 \\ 0 & 8 \end{bmatrix}, \quad R = \begin{bmatrix} 2 \times 10^5 & 0 \\ 0 & 500 \end{bmatrix},$$

$$S = 4R. \quad (28)$$

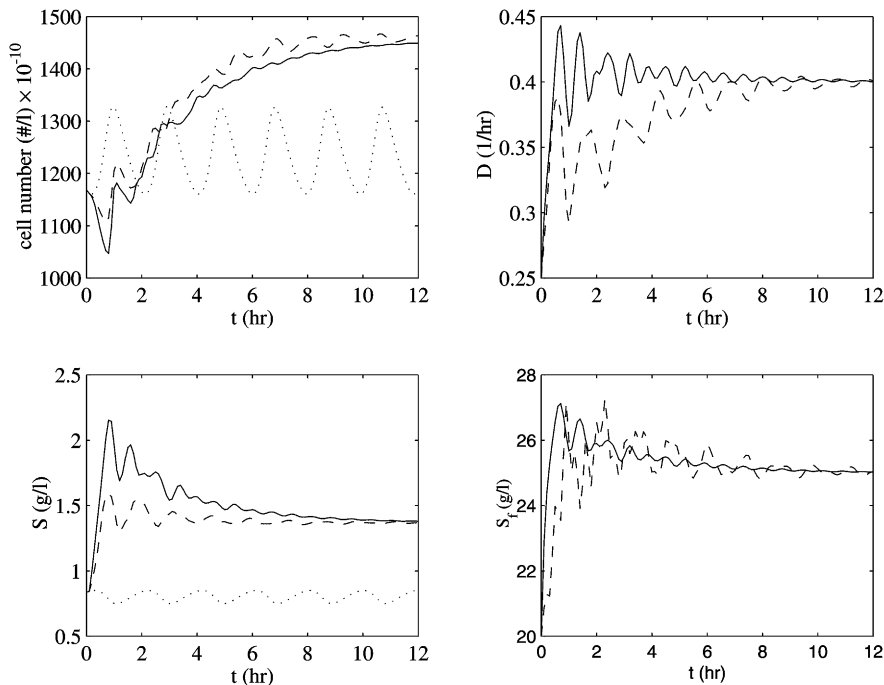


Fig. 7. Oscillation attenuation: full-order output vector with (—) and without (---) disturbance model and open-loop response (···).

Each controller is evaluated with and without disturbance models.

Fig. 7 shows the ability of the MPC controller based on the full-order output vector to stabilize an initially oscillating culture at a desired steady-state operating point. The initial cell number distribution $W(m, 0)$ is a highly synchronized distribution corresponding to the stable periodic solution in Fig. 6, while the discretized cell distribution setpoint vector represents the steady-state solution in Fig. 6. The zeroth-order moment of the cell number distribution, $w_0 = \int_0^\infty W(m, t) dm$, and the substrate concentration are shown as representative output variables. The MPC response with disturbance model is shown by the dashed line, while the solid line represents the response without disturbance model. The MPC controller is able to stabilize the reactor under initial conditions that lead to open-loop oscillations shown by the dotted line. The input and output responses of the MPC controller with disturbance model are more oscillatory than those obtained without the disturbance model. Although the performance may be improved by further fine tuning, the behavior is directly attributable to the additional dynamics introduced by the linear observer used to estimate the disturbances.

Fig. 8 shows the results obtained for the MPC controller with reduced-order output vector for the same test as in Fig. 7. The solid line is the MPC response, while the dashed line is the open-loop response obtained with the synchronized initial cell distribution. While the output responses are only slightly better than those in Fig. 7, the MPC controller with reduced-order output vector provides much smoother input moves. We believe this

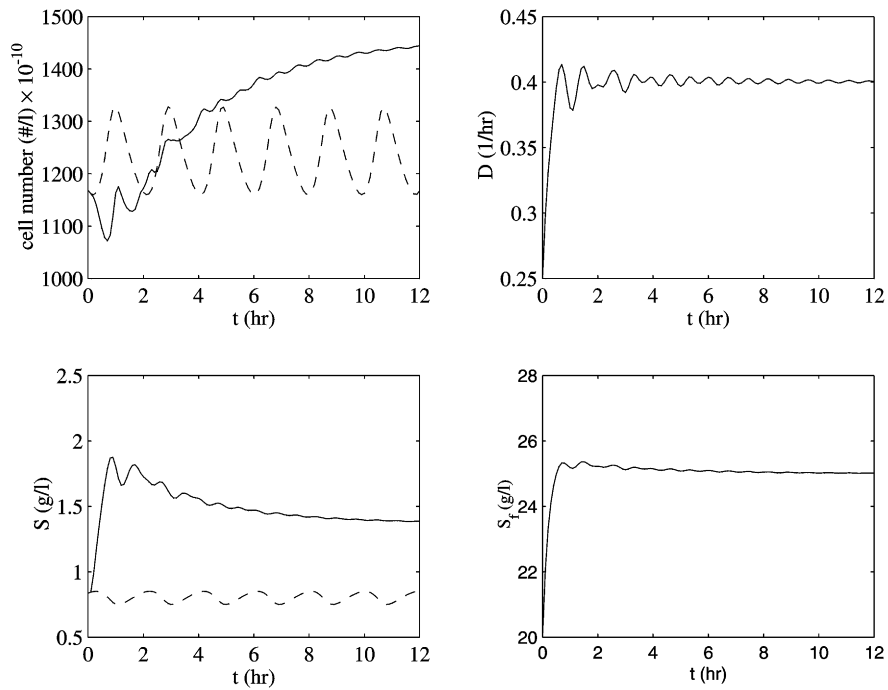


Fig. 8. Oscillation attenuation: reduced-order output vector without disturbance model (—) and open-loop response (---).

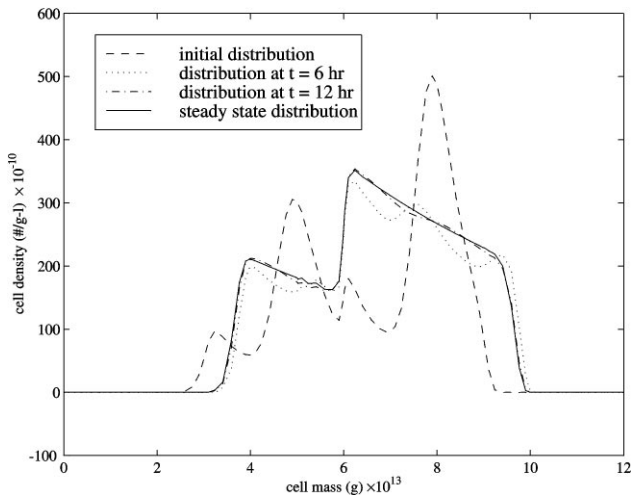


Fig. 9. Oscillation attenuation: cell number distribution corresponding to Fig. 8 at four time instances.

behavior is a direct result of reducing the controlled output vector dimension and making the control problem less nonsquare. The associated time evolution of the cell number distribution is shown in Fig. 9. The initial distribution is a highly synchronized with distinct subpopulations that lead to sustained oscillations. The controller attenuates the oscillations by counteracting cell synchrony via dispersion of the subpopulations. The distribution approaches the desired steady-state distribution by the end of the 12 h simulation.

We further evaluate the effect of the disturbance model on closed-loop performance when a modeling error is present. The modeling error is introduced by changing the cell growth rate parameter K_m from 25 to 20 g/l in the simulated plant, while the linear controller design model remains unchanged. Fig. 10 shows the results obtained for the same oscillation attenuation test as in Figs. 7 and 8. The response of the MPC controller with reduced-order output vector and disturbance model is shown by the solid line, while the dashed line is the response of the same MPC controller without disturbance model. Both controllers are able to attenuate the oscillations and drive the cell distribution to steady state. A notable difference is that input responses for the controller without disturbance model are much smoother. Another difference is that the controllers achieve two very different steady states. The distributions at $t = 24$ h shown in Fig. 11 show a potential advantage of the disturbance model. While the steady-state distribution obtained without the disturbance model (dashed line) is shifted from the setpoints (+), the distribution obtained with the disturbance model (solid line) matches the setpoints almost exactly. The disturbance model is useful only if precise control of the cell number distribution is required. This may be beneficial, for example, if desired metabolites are preferentially produced by cells of a certain mass.

Fig. 12 shows the ability of the MPC controller with reduced-order output vector to stabilize a desired periodic solution. A disturbance model is not used for this test. The initial cell number distribution corresponds to

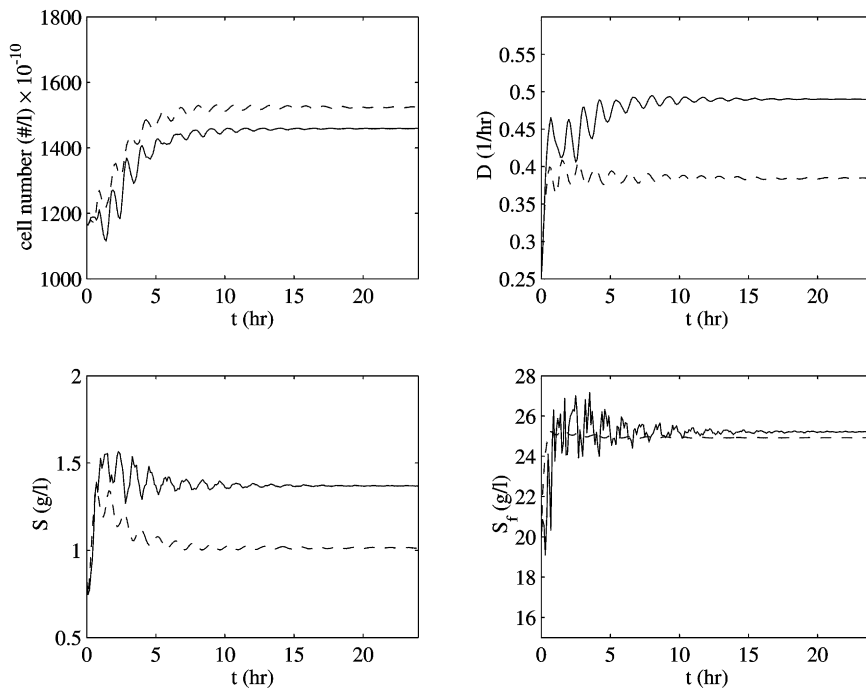


Fig. 10. Oscillation attenuation with modeling error: reduced-order output vector with (—) and without (---) disturbance model.

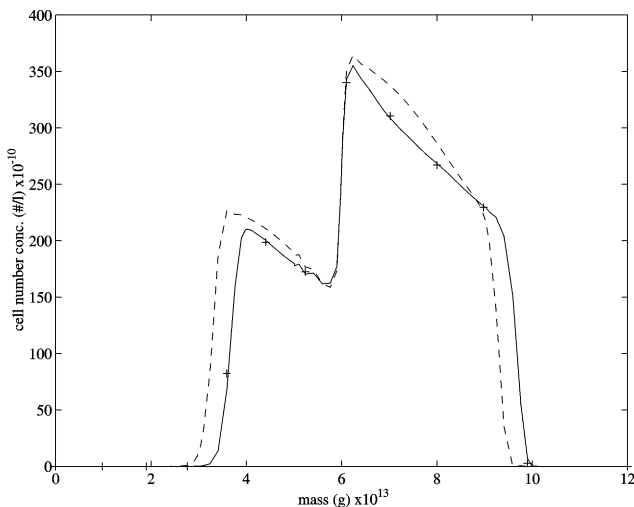


Fig. 11. Oscillation attenuation with modeling error: distribution setpoint (+), reduced-order output vector with (—) and without (---) disturbance model corresponding to Fig. 10.

a steady-state solution, while distributions corresponding to the periodic solution in Fig. 6 are defined as a time-varying setpoint trajectory. For this test, the weighting matrices are chosen by trial-and-error as

$$Q = \begin{bmatrix} 0.01 I_{13 \times 13} & 0 \\ 0 & 10 \end{bmatrix}, \quad R = \begin{bmatrix} 10^5 & 0 \\ 0 & 100 \end{bmatrix}, \quad S = 2R. \quad (29)$$

Note that the controller stabilizes the desired periodic solution by generating oscillatory input moves. Although not shown, it is interesting to note that the observed oscillations are maintained with the same period when the controller is switched off and the system runs under open-loop conditions. The evolution of the cell number distribution is shown in Fig. 13. Clearly the oscillating dynamics of the cell culture is accompanied by marked synchronization of the cell population. Two distinct sub-populations can be identified after 24 h of operation.

5. Summary

The dynamic model for the continuous yeast bioreactor is formulated by coupling the population balance equations (PBE) for the cell mass distribution to the substrate mass balance. We have shown that empirical functions used to describe the dependence of cell transition and division on the medium can be chosen such that the PBE model exhibits stable periodic solutions under reasonable operating conditions. The model is solved numerically by spatially discretizing the PBE using orthogonal collocation on finite elements. The resulting nonlinear ordinary differential equation model is linearized and discretized in time to yield a linear state-space model suitable for MPC synthesis. The MPC controller is designed to stabilize steady-state and periodic solutions by regulating the discretized cell number distribution and the substrate concentration. Several

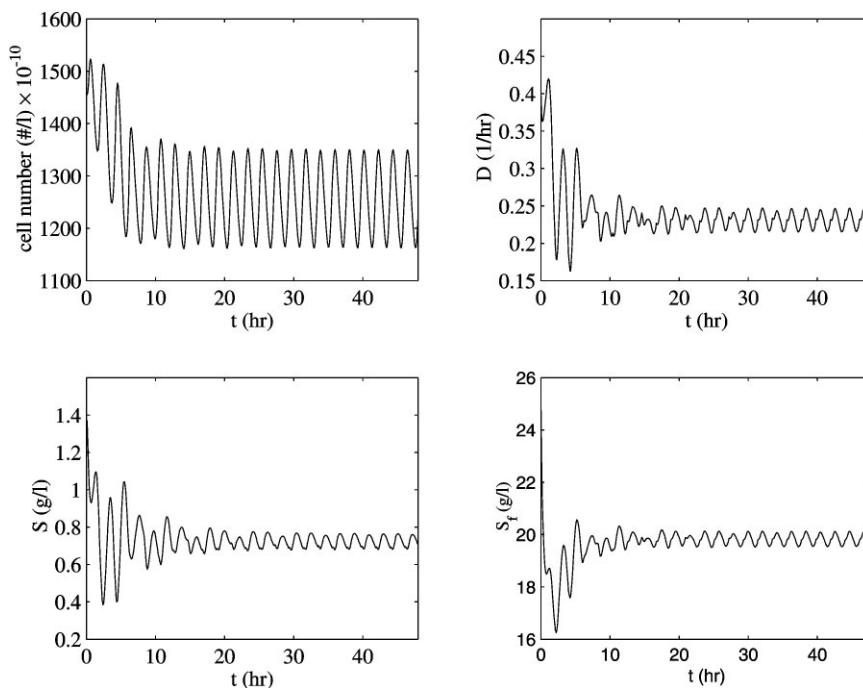


Fig. 12. Oscillation induction.

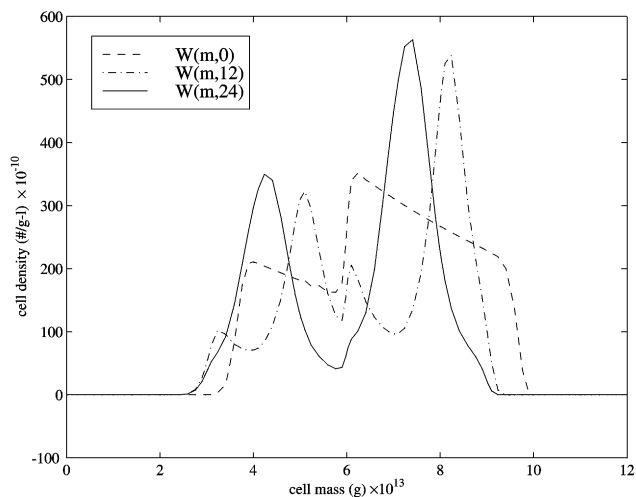


Fig. 13. Oscillation induction: synchronization of the cell distribution corresponding to Fig. 12.

MPC formulations have been evaluated via simulation. The best results are obtained when a subset of the discretized cell number distribution is used as the controlled outputs. The proposed methodology is the initial step in the development of an implementable control strategy for oscillating yeast cultures.

Acknowledgements

Financial support from the National Science Foundation (Grants CTS-9501368 and BES-9522274) is gratefully acknowledged.

References

- Alberghina, L., Ranzi, B. M., Porro, D., & Martegani, E. (1991). Flow cytometry and cell cycle kinetics in continuous and fed-batch fermentations of budding yeast. *Biotechnology Progress*, 7, 299–304.
- Bakken, L. R., & Olsen, R. A. (1983). Buoyant densities and dry-matter contents of microorganisms: Conversion of a measured biovolume into biomass. *Applied Environmental Microbiology*, 45, 1188–1195.
- Beuse, M., Bartling, R., Kopmann, A., Diekmann, H., & Thoma, M. (1998). Effect of the dilution rate on the mode of oscillation in continuous cultures of *Saccharomyces cerevisiae*. *Journal of Biotechnology*, 61, 15–31.
- Cazzador, L., Mariani, L., Martegani, E., & Alberghina, L. (1990). Structured segregated models and analysis of self-oscillating yeast continuous cultures. *Bioprocess Engineering*, 5, 175–180.
- Chen, C.-I., & McDonald, K. A. (1990). Oscillatory behavior of *Saccharomyces cerevisiae* in continuous culture: II. Analysis of cell synchronization and metabolism. *Biotechnology and Bioengineering*, 36, 28–38.
- Chiu, T., & Christofides, P. D. (1999). Nonlinear control of particulate processes. *A.I.Ch.E. Journal*, 45, 1279–1297.
- Clarke-Pringle, T., & MacGregor, J. F. (1998). Product quality control in reduced dimensional spaces. *Industrial and Engineering Chemistry Research*, 37, 3992–4002.
- Eaton, J. W., & Rawlings, J. B. (1990). Feedback control of chemical processes using on-line optimization techniques. *Computers & Chemical Engineering*, 14, 469–479.
- Finlayson, B. A. (1980). *Nonlinear analysis in chemical engineering*. New York, NY: McGraw-Hill.
- Heffels, C., Polke, R., Radle, M., Sachweb, B., Schaffer, M., & Scholz, N. (1998). Control of particulate processes by optical measurement techniques. *Particle and Particle Systems Character*, 15, 211–218.
- Hjortso, M. (1987). Periodic forcing of microbial cultures. A model for induction synchrony. *Biotechnology and Bioengineering*, 30, 825–835.
- Hjortso, M. (1996). Population balance models of autonomous periodic dynamics in microbial cultures. Their use in process optimization. *Canadian Journal of Chemical Engineering*, 74, 612–620.

- Hjortso, M., & Bailey, J. (1983). Transient responses of budding yeast populations. *Mathematical Biosciences*, *63*, 121–148.
- Hjortso, M., & Nielsen, J. (1994). A conceptual model of autonomous oscillations in microbial cultures. *Chemical Engineering Science*, *49*, 1083–1095.
- Hjortso, M., & Nielsen, J. (1995). Population balance models of autonomous microbial oscillations. *Journal of Biotechnology*, *42*, 255–269.
- Jones, K. D., & Kompala, D. S. (1999). Cybernetic model of the growth dynamics of *Saccharomyces cerevisiae* in batch and continuous cultures. *Journal of Biotechnology*, *71*, 105–131.
- Kalani, A., & Christofides, P. D. (1999). Nonlinear control of spatially inhomogeneous aerosol processes. *Chemical Engineering Science*, *54*, 2669–2678.
- Kurtz, M. J., Zhu, G. Y., Zamamiri, A. M., Henson, M. A., & Hjortso, M. A. (1998). Control of oscillating microbial cultures described by population balance models. *Industrial and Engineering Chemistry Research*, *37*, 4059–4070.
- Martegani, E., Porro, D., Ranzi, B. M., & Alberghina, L. (1990). Involvement of a cell size control mechanism in the induction and maintenance of oscillations in continuous cultures of budding yeast. *Biotechnology and Bioengineering*, *36*, 453–459.
- McLellan, P. J., Daugulis, A. J., & Li, J. (1999). The incidence of oscillatory behavior in the continuous fermentation of *Zymomonas mobilis*. *Biotechnology Progress*, *15*, 667–680.
- Muske, K. R., & Rawlings, J. B. (1993). Linear model predictive control of unstable processes. *Journal of Process and Control*, *3*, 85–96.
- Rawlings, J. B., Miller, S. M., & Witkowski, W. R. (1993). Model identification and control of solution crystallization processes: A review. *Industrial and Engineering Chemistry Research*, *32*, 1275–1296.
- Rawlings, J. B., Witkowski, W. R., & Eaton, J. W. (1989). Control issues arising in population balance models. *Proceedings of American control conference* (pp. 677–682).
- Rice, R. G., & Do, D. D. (1995). *Applied mathematics and modeling for chemical engineers*. New York, NY: Wiley.
- Robertson, B. R., Button, D. K., & Koch, A. L. (1998). Determination of the biomasses of small bacteria at low concentration in a mixture of species with forward light scatter measurements by flow cytometry. *Applied Environmental Microbiology*, *64*, 3900–3909.
- Semino, D., & Ray, W. H. (1995a). Control of systems described by population balance equations — I. Controllability analysis. *Chemical Engineering Science*, *50*, 1805–1824.
- Semino, D., & Ray, W. H. (1995b). Control of systems described by population balance equations — II. Emulsion polymerization with constrained control action. *Chemical Engineering Science*, *50*, 1825–1839.
- Stephens, M. L., & Lyberatos, G. (1987). Effect of cycling on final mixed culture fate. *Biotechnology and Bioengineering*, *29*, 672–678.
- Strässle, C., Sonnleitner, B., & Feichter, A. (1989a). A predictive model for the spontaneous synchronization of *Saccharomyces cerevisiae* grown in a continuous culture. I. Concept. *Journal of Biotechnology*, *7*, 299–318.
- Strässle, C., Sonnleitner, B., & Feichter, A. (1989b). A predictive model for the spontaneous synchronization of *Saccharomyces cerevisiae* grown in a continuous culture. II. Experimental verification. *Journal of Biotechnology*, *9*, 191–208.
- Yamashit, Y., Kuwashim, M., Nonaka, T., & Suzuki, M. (1993). Online measurement of cell-size distribution and concentration of yeast by image-processing. *Journal of the Chemical Engineering of Japan*, *26*, 615–619.
- Zamamiri, A. M. (1998). *Analysis of oscillating yeast cultures*. Master thesis, Louisiana State University, Baton Rouge, LA.